Endothelium and NOTCH specify and amplify aorta-gonad-mesonephros–derived hematopoietic stem cells

Brandon K. Hadland,[1,2] Barbara Varnum-Finney,[1] Michael G. Poulos,[3,4,5] Randall T. Moon,[6,7] Jason M. Butler,[3,4,5] Shahin Rafii,[3,4,7] and Irwin D. Bernstein[1,2]

[1]Clinical Research Division, Fred Hutchinson Cancer Research Center, Seattle, Washington, USA. [2]Department of Pediatrics, University of Washington School of Medicine, Seattle, Washington, USA. [3]Department of Genetic Medicine, [4]Ansary Stem Cell Institute, [5]Department of Surgery, Weill Cornell Medical College, New York, New York, USA. [6]Department of Pharmacology, Institute for Stem Cell and Regenerative Medicine, University of Washington School of Medicine, Seattle, Washington, USA. [7]Howard Hughes Medical Institute.

Hematopoietic stem cells (HSCs) first emerge during embryonic development within vessels such as the dorsal aorta of the aorta-gonad-mesonephros (AGM) region, suggesting that signals from the vascular microenvironment are critical for HSC development. Here, we demonstrated that AGM-derived endothelial cells (ECs) engineered to constitutively express AKT (AGM AKT-ECs) can provide an in vitro niche that recapitulates embryonic HSC specification and amplification. Specifically, nonengrafting embryonic precursors, including the VE-cadherin–expressing population that lacks hematopoietic surface markers, cocultured with AGM AKT-ECs specified into long-term, adult-engrafting HSCs, establishing that a vascular niche is sufficient to induce the endothelial-to-HSC transition in vitro. Subsequent to hematopoietic induction, coculture with AGM AKT-ECs also substantially increased the numbers of HSCs derived from VE-cadherin$^+$CD45$^+$ AGM hematopoietic cells, consistent with a role in supporting further HSC maturation and self-renewal. We also identified conditions that included NOTCH activation with an immobilized NOTCH ligand that were sufficient to amplify AGM-derived HSCs following their specification in the absence of AGM AKT-ECs. Together, these studies begin to define the critical niche components and resident signals required for HSC induction and self-renewal ex vivo, and thus provide insight for development of defined in vitro systems targeted toward HSC generation for therapeutic applications.

Introduction

In the developing embryo, the earliest hematopoietic activity is characterized by lineage-restricted progenitors that arise initially in the yolk sac prior to and independent of hematopoietic stem cells (HSCs) (1–4). In contrast, the first definitive HSCs — defined by their capacity for long-term, multilineage engraftment in adult recipients — are detected thereafter in arterial vessels, such as the dorsal aorta, of the region known as the aorta-gonad-mesonephros (AGM) (5) and subsequently home to the fetal liver, where HSCs undergo further maturation and significant proliferative expansion prior to seeding the marrow (6, 7). Importantly, identifying the resident niche signals that distinctly support the specification and initial self-renewal of definitive HSCs could improve our ability to generate transplantable HSCs from pluripotent stem cells or reprogrammed cells, and thus have significant therapeutic implications.

The transition to definitive HSCs occurs from VE-cadherin$^+$ endothelial-like precursors called hemogenic endothelium (HE) in the context of the arterial vasculature via maturation through HSC precursors (8, 9), suggesting the vascular niche provides signals for HSC induction from HE. While HE cells are phenotypically indistinguishable by most known surface markers from nonhemogenic endothelial cells (ECs), they express hematopoietic transcription factors, such as RUNX1, during the endothelial-to-HSC transition (10, 11). Recently, this transition has been visualized in the dorsal aorta as clusters of hematopoietic cells (expressing initial hematopoietic markers c-KIT and CD41, followed by CD45) bud from the underlying endothelium within the vascular wall (12–14), suggesting dynamic interactions between emerging hematopoietic cells and cells of the vascular niche regulate the process of HSC formation. Importantly, the niche must provide signals that not only promote HSC induction from HE, but subsequently limit lineage-restricted differentiation and promote HSC self-renewal. Notably, signals to support HSC amplification are present in AGM explant or reaggregation cultures ex vivo; These signals were shown to correlate with survival of ECs (15, 16). The capacity of primary ECs from the paraaortic splanchnopleura (P-Sp) — the mesodermal precursor to the AGM region — to support HSC activity from adult BM during in vitro coculture was demonstrated by Li and colleagues (17), while other studies have shown that stromal cell lines derived from the AGM region, some of which have endothelial properties, can support both embryonic and adult HSC maintenance in vitro (18–20). Furthermore, previous studies from our labs and others have established a role for the vascular niche in supporting adult marrow–derived HSCs ex vivo (21–24). However, it has not previously been established whether an EC niche, such as from the AGM, is sufficient to induce the specification of bona fide, long-term engrafting HSCs from nonengrafting embryonic precursors, including HE, and support subsequent numerical expansion of embryonic-stage HSCs.

Within the AGM, NOTCH signaling is essential for HSC development and is thought to be mediated by cell-to-cell interactions involving dynamic NOTCH receptor expression on hematopoietic

Conflict of interest: The authors have declared that no conflict of interest exists.
Submitted: November 21, 2014; **Accepted:** March 5, 2015.
Reference information: *J Clin Invest*. 2015;125(5):2032–2045. doi:10.1172/JCI80137.

cells emerging from underlying ECs expressing NOTCH ligands (25). Whereas NOTCH signaling is dispensable for the earlier yolk sac–derived primitive and erythromyeloid phases of hematopoiesis, knockout and chimeric analysis in murine embryos demonstrated that NOTCH1 signaling is required for definitive HSCs that can contribute to long-term multilineage hematopoiesis (26, 27). In this context, NOTCH1 activation is known to play a role in arterial endothelial fate and in embryonic HSC specification mediated via downstream transcription factors such as GATA2, HES1, and RUNX1 (28–31). Notably, a recent study also suggests a function for NOTCH1 signaling supporting fetal liver HSCs (32), a unique period when HSCs are undergoing substantial proliferative expansion. Although canonical NOTCH signaling does not appear to be required for adult HSCs during homeostasis (33), NOTCH2 activation may promote HSC self-renewal by limiting their differentiation under certain proliferative conditions, such as after BM injury (34). Thus, NOTCH activation mediated by ligand expression within cells of various hematopoietic niches may play a role in supporting multiple phases of HSC development from specification to self-renewal. Further understanding of the effects of stage-specific NOTCH activation in nascent HSCs and their precursors from the AGM may increase our ability to generate HSCs ex vivo.

To dissect the niche requirements for embryonic HSC development, we describe here the use of ECs derived from the AGM as a substrate to recapitulate early HSC specification and amplification in vitro. We utilized primary AGM ECs in which constitutive AKT activation was induced to generate an in vitro vascular niche suitable for coculture in serum-free conditions, and show that AKT-activated AGM-derived ECs (AGM AKT-ECs) provide signals sufficient to promote induction of engrafting HSCs from non-engrafting embryo-derived precursors, including HE. Furthermore, these ECs enhance subsequent expansion of HSC numbers from specified VE-cadherin$^+$CD45$^+$ hematopoietic cells from the AGM. We further identified conditions with NOTCH activation, cytokines, and TGF-β inhibition that were sufficient to support an increase of AGM-derived, long-term HSCs but were insufficient in generating HSCs from HE. Altogether, these studies begin to deconstruct the necessary conditions to promote induction and self-renewal of HSCs ex vivo, which will further the goal of developing methods using defined reagents to generate HSCs in vitro for therapeutic purposes.

Results

AGM-derived ECs are sustained in culture by induced AKT activation and express NOTCH ligands. Based on the close association of emerging hematopoietic cells in the AGM with the underlying arterial endothelium, we sought to test whether AGM-derived ECs could provide an in vitro substrate for HSC induction and self-renewal. To generate ECs from the AGM region, we cultured sorted VE-cadherin$^+$CD45$^-$ or VE-cadherin$^+$CD45$^-$CD41$^-$ cells from dissociated AGM dissected from embryonic day 10–11 (E10–E11) embryos in endothelial-supportive media to generate colonies of VE-cadherin$^+$CD31$^+$ cells (Figure 1, A and B). AGM-derived ECs were sustained in culture by infection with a lentivirus encoding constitutively active AKT1 (myristoylated AKT1; MyrAKT) (23). This method has been used to culture primary ECs from other organs, promoting EC survival in serum/growth factor–free conditions to study EC contribution to stem/progenitor cell niches in vitro (35). AGM AKT-ECs express endothelial markers VE-cadherin, CD31, and FLK1 — as well as SCA-1 and low levels of CD34 — and lack expression of hematopoietic marker CD45 (Figure 1B). Furthermore, AGM AKT-ECs demonstrate relatively homogenous expression of NOTCH ligands, including Jagged1 (JAG1), Jagged2 (JAG2), Delta-like-1 (DLL1), and Delta-like-4 (DLL4) (characteristic of arterial endothelium), compared with more heterogeneous expression of NOTCH ligands on fresh AGM ECs (gated as VE-cadherin$^+$CD45$^-$CD41$^-$) from dissected embryos (Figure 1C; control staining in Supplemental Figure 1; supplemental material available online with this article; doi:10.1172/JCI80137DS1). Although the population from which AGM AKT-ECs are derived may contain a small proportion of HE cells at the time they are isolated that cannot be distinguished by known surface markers, we observed no residual hematopoietic potential of the AGM AKT-ECs once established, as assayed by generation of phenotypic CD45$^+$ cells, hematopoietic colony-forming potential, or transplantation assays following culture of AGM AKT-ECs alone with hematopoietic cytokines (AGM AKT-EC only), in experiments performed in parallel with coculture experiments described below (Figure 2 and data not shown).

AGM-derived EC coculture induces HSCs from E9–E10 VE-cadherin$^+$ precursors. Previous studies demonstrated that HSC activity can be detected in the AGM at low frequency (3 mice engrafted from 112 embryos) as early as E10.5 (34–41 somite pairs [sp]) by direct transplantation to adult recipients (5). Prior to this stage, between E9 and E10, in vitro multipotent hematopoietic progenitors and precursors capable of engraftment into conditioned newborn mice can be detected in the VE-cadherin$^+$ and c-KIT$^+$ populations (36, 37), suggesting that further maturation from precursors before E10.5 is required prior to attaining the capacity for multilineage engraftment into adult recipients. To determine whether AGM AKT-ECs can promote HSC induction from developmental precursors, we isolated VE-cadherin$^+$ cells from E9.5–E10 (25–32 sp) P-Sp/AGM for coculture in the presence of serum-free media (X-Vivo) and hematopoietic cytokines (TPO, SCF, IL3, FLT3L) (Figure 2A). Sorted E9.5–E10 VE-cadherin$^+$ cells gave rise visually to colonies of apparent hematopoietic cells during coculture on AGM AKT-ECs (Figure 2B). Hematopoietic identity of cells generated in coculture was confirmed by FACS demonstrating surface expression of the pan-hematopoietic marker CD45$^+$ (Figure 2C). A subset of cells also expressed markers of myeloid lineage (Gr1 and F4/80), erythroid lineage (TER119), and stem/progenitor cells (LSK phenotype: SCA-1$^+$, c-KIT$^+$, lineage marker–negative) (Supplemental Figure 2). Compared with the initial VE-cadherin$^+$ precursor population and with cells cultured under control conditions without ECs, cells cultured on AGM AKT-ECs generated enhanced numbers of total hematopoietic cells, LSK stem/progenitor cells, and colony-forming progenitors (Figure 2, D and E). Most importantly, E9.5–E10 P-Sp/AGM VE-cadherin$^+$ cells cultured on AGM AKT-ECs also generated HSCs capable of high-level, multilineage engraftment at more than 20 weeks after transplant in peripheral blood (PB), BM, thymus, and spleen of transplanted adult congenic-strain mice. These HSCs were also capable of multilineage engraftment following transplantation into secondary recipients (Figure 2, F and G, and Supplemental Figure 3A). Similar high-

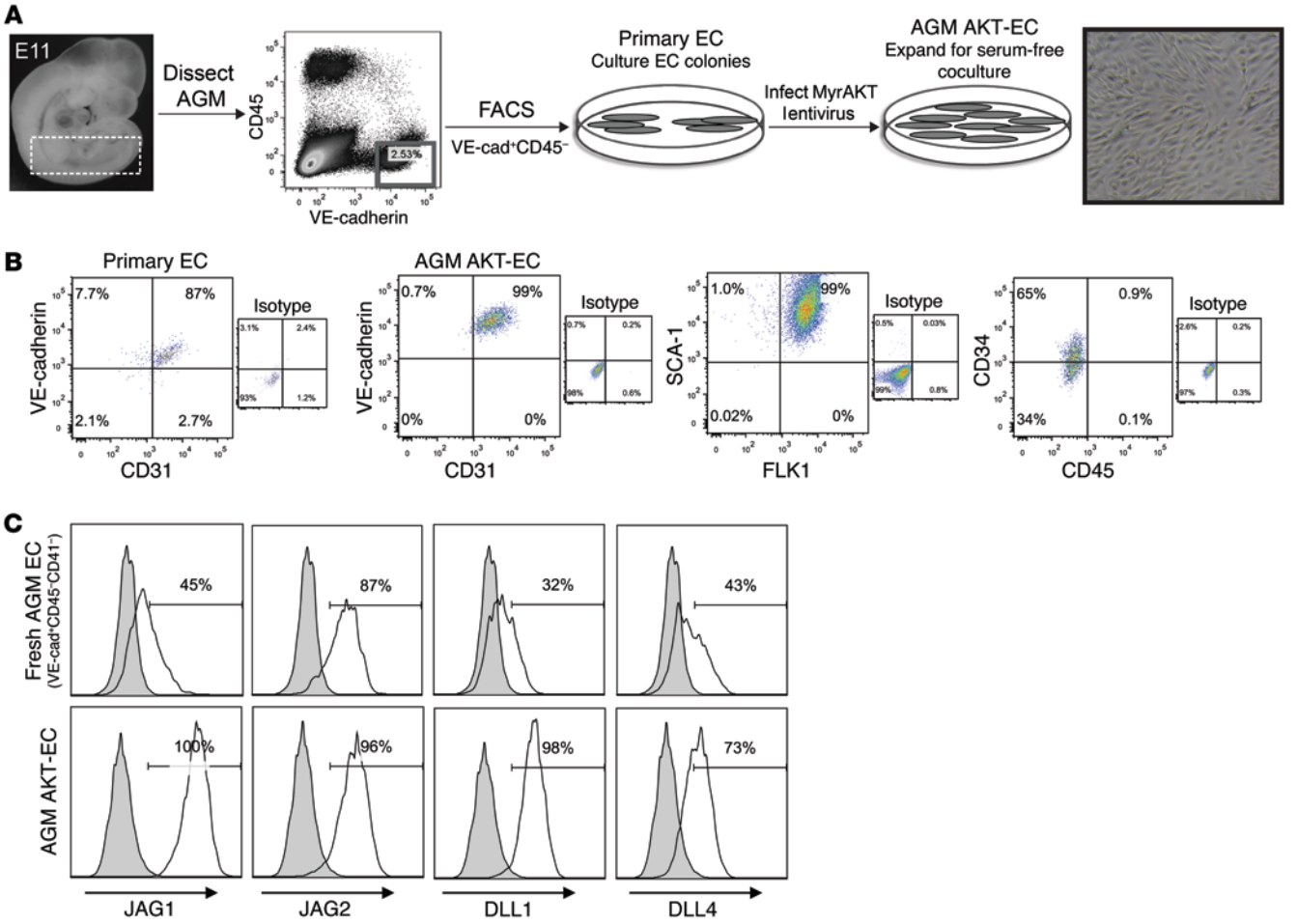

Figure 1. Constitutive AKT expression permits culture of AGM AKT-EC –expressing NOTCH ligands. (**A**) Schematic of method for generation of AGM AKT-ECs. Image of cultured AGM AKT-ECs, magnification ×100. Dotted box indicates approximate region of the AGM. (**B**) Surface expression of endothelial markers VE-cadherin and CD31 on primary EC colonies cultured from AGM region and in AGM AKT-ECs following MyrAKT lentiviral transduction and expansion. Surface expression of FLK1, SCA-1, CD34, and CD45 in AGM AKT-ECs. Sub-plots show EC staining with isotype control antibodies. (**C**) Surface expression of NOTCH ligands JAG1, JAG2, DLL1, and DLL4, and corresponding isotype controls (shown in gray) on freshly sorted AGM endothelium (gated as VE-cadherin$^+$CD45$^-$CD41$^-$) and AGM AKT-ECs.

level, multilineage engraftment was observed from VE-cadherin$^+$ cells cultured with multiple, independently generated AGM AKT-ECs (Figure 2H). Furthermore, VE-cadherin$^+$ cells capable of generating HSCs with long-term, multilineage engraftment into adult mice were detected as early as E9 (13–20 somite pairs [sp]), following 7 days of coculture with AGM AKT-ECs (Figure 2H). In contrast, control cultures without ECs or on OP9, a stromal line that supports hematopoietic progenitor activity in culture (38), did not produce engrafting cells (Figure 2, F and H). As expected, freshly sorted, uncultured VE-cadherin$^+$ cells from E9.5–E10 P-Sp/AGM did not engraft adult recipients, nor did AGM AKT-ECs cultured alone under hematopoietic conditions without P-Sp/AGM cells (Figure 2H). Altogether, these results demonstrate that AGM AKT-ECs express niche factors capable of promoting HSC induction in vitro from nonengrafting VE-cadherin$^+$ precursors.

AGM-derived ECs coculture induces HSCs from E9–E10 HE. Beginning after E9 in the P-Sp/AGM, the VE-cadherin$^+$ population contains both c-KIT$^-$ ECs as well as c-KIT$^+$ hematopoietic progenitor cells (HPCs), which also express low levels of the early hematopoietic marker CD41 (14) (see below). c-KIT/CD41 expression identifies the earliest HSC precursors that can be matured to adult-engrafting HSCs by reaggregation culture (39, 40) or by primary transplantation to conditioned newborn mice (36). The VE-cadherin$^+$c-KIT$^-$ endothelial population contains a small portion of HE not yet expressing hematopoietic surface markers and thus indistinguishable from nonhemogenic ECs at this stage by known surface markers. To determine the subset of VE-cadherin$^+$ cells that could give rise to HSCs, we initially separated VE-cadherin$^+$ cells into VE-cadherin$^+$c-KIT$^+$ HPCs or VE-cadherin$^+$c-KIT$^-$ ECs (containing HE) from E9.5–E10 P-Sp/AGM for coculture (Figure 2A). Notably, both VE-cadherin$^+$c-KIT$^+$ HPCs and VE-cadherin$^+$ c-KIT$^-$ ECs/HE generated engrafting HSCs following AGM AKT-EC coculture (Figure 3A).

While these results suggested the capacity of AGM AKT-ECs to induce HSCs from HE in vitro, further validation was necessary to rule out the possibility of contamination of the VE-cadherin$^+$ c-KIT$^-$ population with HPCs. Thus, we also examined the potential of HE defined by absence of expression of CD41, the earliest

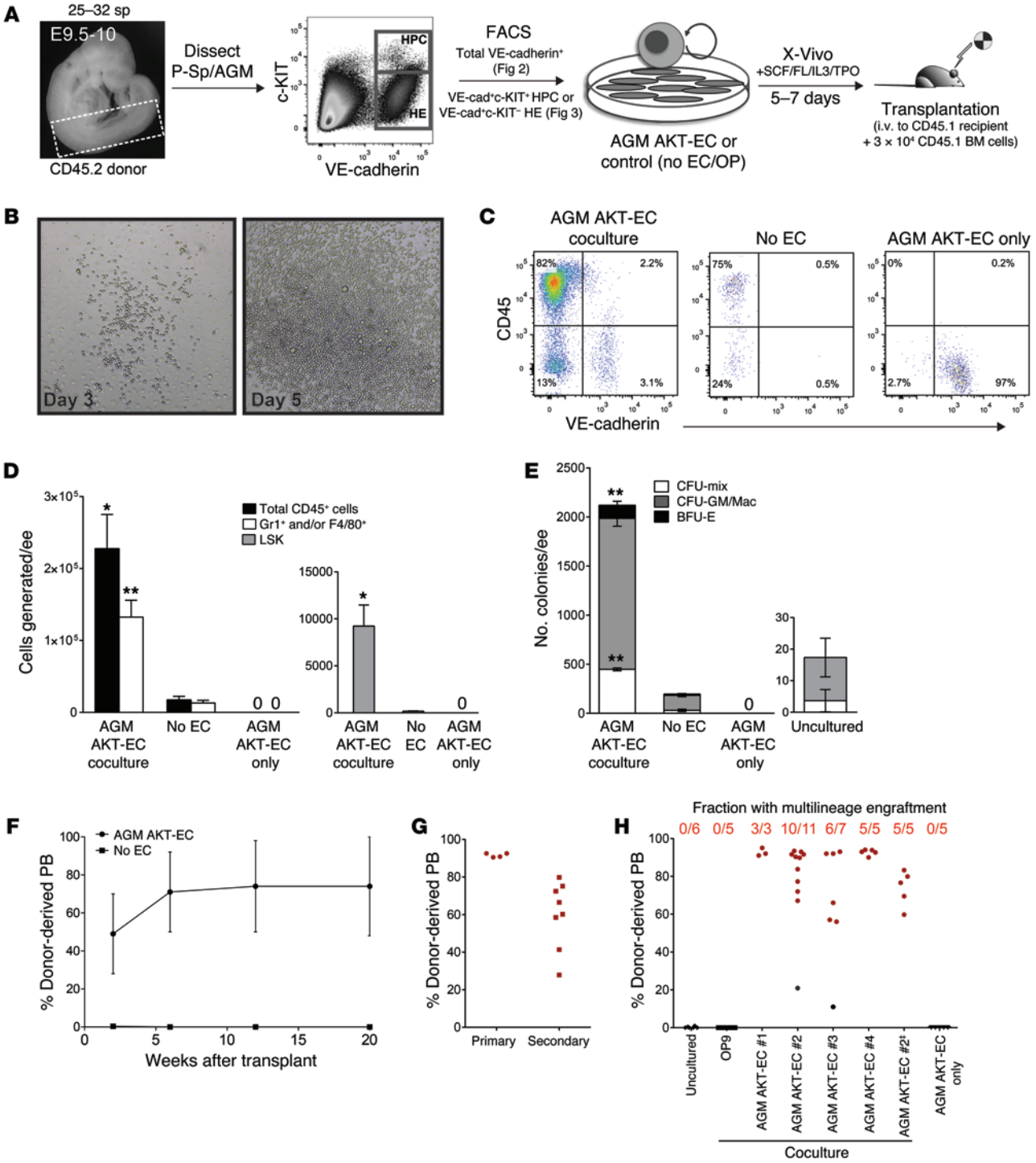

Figure 2. Coculture on AGM AKT-ECs generates long-term HSCs from E9.5–E10 P-Sp/AGM VE-cadherin⁺ precursors. (**A**) Schematic of experimental design. Dotted box indicates approximate region of the P-Sp/AGM. (**B**) Formation of hematopoietic colonies (magnification ×100) and (**C**) CD45⁺ cells from sorted P-Sp/AGM VE-cadherin⁺ cells during coculture with AGM AKT-ECs or without ECs. Also shown are AGM AKT-ECs cultured with hematopoietic cytokines but without P-Sp/AGM cells (AGM AKT-EC only). (**D**) Total CD45⁺, myeloid (Gr1⁺ and/or F4/80⁺), and LSK cells generated per embryo equivalent (ee) of starting cells. Shown is mean ± SD (n = 3), from representative experiment (n = 3). (**E**) CFU progenitors per ee of starting cells. Shown is mean ± SD (n = 3), from representative experiment (n = 2). (**F**) Engraftment of VE-cadherin⁺ cells cultured on AGM AKT-ECs or control (no EC). Shown at each time point is mean ± SD of PB engraftment (n = 4 experiments, 23 total mice), transplanted at 0.5–2 ee. (**G**) Donor-derived PB engraftment at ≥16 weeks from n = 4 primary recipients transplanted to each of 2 secondary recipients. (**H**) Engraftment in PB at ≥16 weeks after transplant from E9.5–E10 VE-cadherin⁺ cells transplanted directly after sort (uncultured) with 2 ee, following coculture on OP9, or on multiple independent AGM AKT-ECs (#1–4) transplanted with 1–2 ee of cells. ‡Transplant from cocultured cells from E9 P-Sp (13–20 sp). Control AGM AKT-ECs cultured with hematopoietic cytokines but without P-Sp/AGM cells were also tested for engraftment (AGM AKT-EC only). Numbers above indicate fraction of mice with multilineage engraftment, designated by data points in red. *P < 0.05, **P < 0.01 AGM, AKT-EC coculture vs. no EC; unpaired Student's t test.

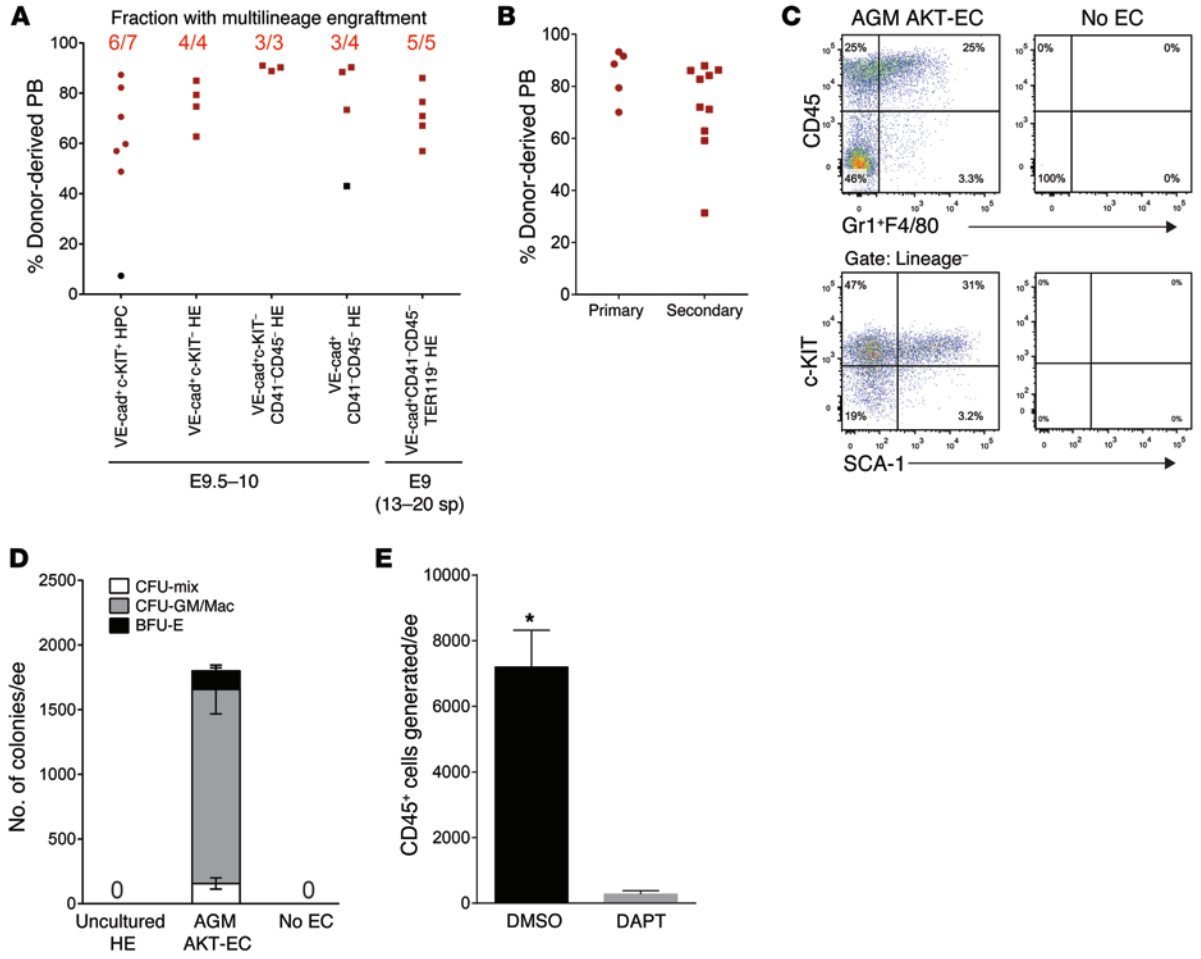

Figure 3. Coculture on AGM AKT-ECs generates long-term HSCs from both hematopoietic progenitor cells and HE. (**A**) Engraftment in PB at ≥16 weeks after transplant from VE-cadherin$^+$c-KIT$^+$ HPCs or HE sorted as indicated (see also Supplemental Figure 4 for sorting windows and after-sort analysis), following coculture on AGM AKT-ECs, each transplanted with 1–2 embryo equivalent (ee) of cells. Numbers above indicate fraction of mice with multilineage engraftment, designated by data points in red. (**B**) Donor-derived PB engraftment at ≥16 weeks from n = 5 primary recipients (transplanted with AGM AKT-cultured HE cells) transplanted to each of 2 secondary recipients. (**C**) CD45$^+$, myeloid (Gr1$^+$ and/or F4/80$^+$), and LSK cells generated from P-Sp/AGM VE-cadherin$^+$ CD41$^-$CD45$^-$ HE following coculture with AGM AKT-ECs or without AGM AKT-ECs (no EC). (**D**) CFU progenitors per ee of HE cells, freshly sorted (uncultured HE), following AGM AKT-EC culture, or cultured without ECs (no EC). Shown is mean ± SD of CFU (n = 3), from representative experiment (n = 2). (**E**) Total CD45$^+$ hematopoietic cells generated from HE following AGM AKT-EC coculture in the presence of DMSO (carrier control) or gamma-secretase inhibitor DAPT. Shown is mean ± SD from replicate samples (n = 3), from representative experiment (n = 3). (*P < 0.001, DMSO vs. DAPT, unpaired Student's t test).

marker of HPCs with clonal colony-forming capacity in the P-Sp/AGM, and CD45, a pan-hematopoietic marker expressed subsequent to CD41 in P-Sp/AGM HPCs. We observed long-term, multilineage primary and secondary engraftment from either VE-cadherin$^+$c-KIT$^-$CD45$^-$CD41$^-$ or VE-cadherin$^+$CD41$^-$CD45$^-$ HE from E9.5–E10 P-Sp/AGM following 5–6 days AGM AKT-EC coculture, as well as from VE-cadherin$^+$CD41$^-$CD45$^-$TER119$^-$ HE from E9 (13–20 sp) P-Sp/AGM following 7 days of coculture (Figure 3, A and B, and Supplemental Figure 4, A–C).

The HE-to-hematopoietic transition is dependent on extrinsic niche signals that include NOTCH pathway activation mediated by NOTCH ligand–expressing stromal cells. In the absence of such inductive signals, HE by definition should lack direct clonal hematopoietic activity. Consistent with this, VE-cadherin$^+$CD41$^-$CD45$^-$ HE cells sorted from E9.5–E10 P-Sp/AGM contain no direct CFU progenitor activity in methylcellulose assays and are unable to generate CD45$^+$ hematopoietic cells or CFU progenitors following culture with media and cytokines in the absence of stroma. However, AGM AKT-ECs can induce generation of CD45$^+$ cells — including myeloid cells expressing Gr-1 or F4/80, and LSK stem/progenitor cells — and CFU progenitors from HE following coculture (Figure 3, C and D).

Since NOTCH is an essential pathway involved in the endothelial-to-hematopoietic transition in the P-Sp/AGM at this stage, we also tested whether blocking NOTCH signaling could inhibit hematopoietic induction from HE upon AGM AKT-EC coculture. Consistent with a requirement for NOTCH, we show that generation of CD45$^+$ cells from VE-cadherin$^+$CD41$^-$CD45$^-$ HE cultured on AGM AKT-ECs was significantly reduced by the addition of the gamma-secretase inhibitor DAPT, which blocks NOTCH activation by preventing cleavage of the intracellular domain required for downstream signaling through NOTCH receptors (Figure 3E). We also tested hematopoietic-supportive OP9 stromal cells (endogenously expressing NOTCH ligand JAG1) or OP9 cells engineered to express NOTCH ligands DLL1 or DLL4 (Supplemental Figure

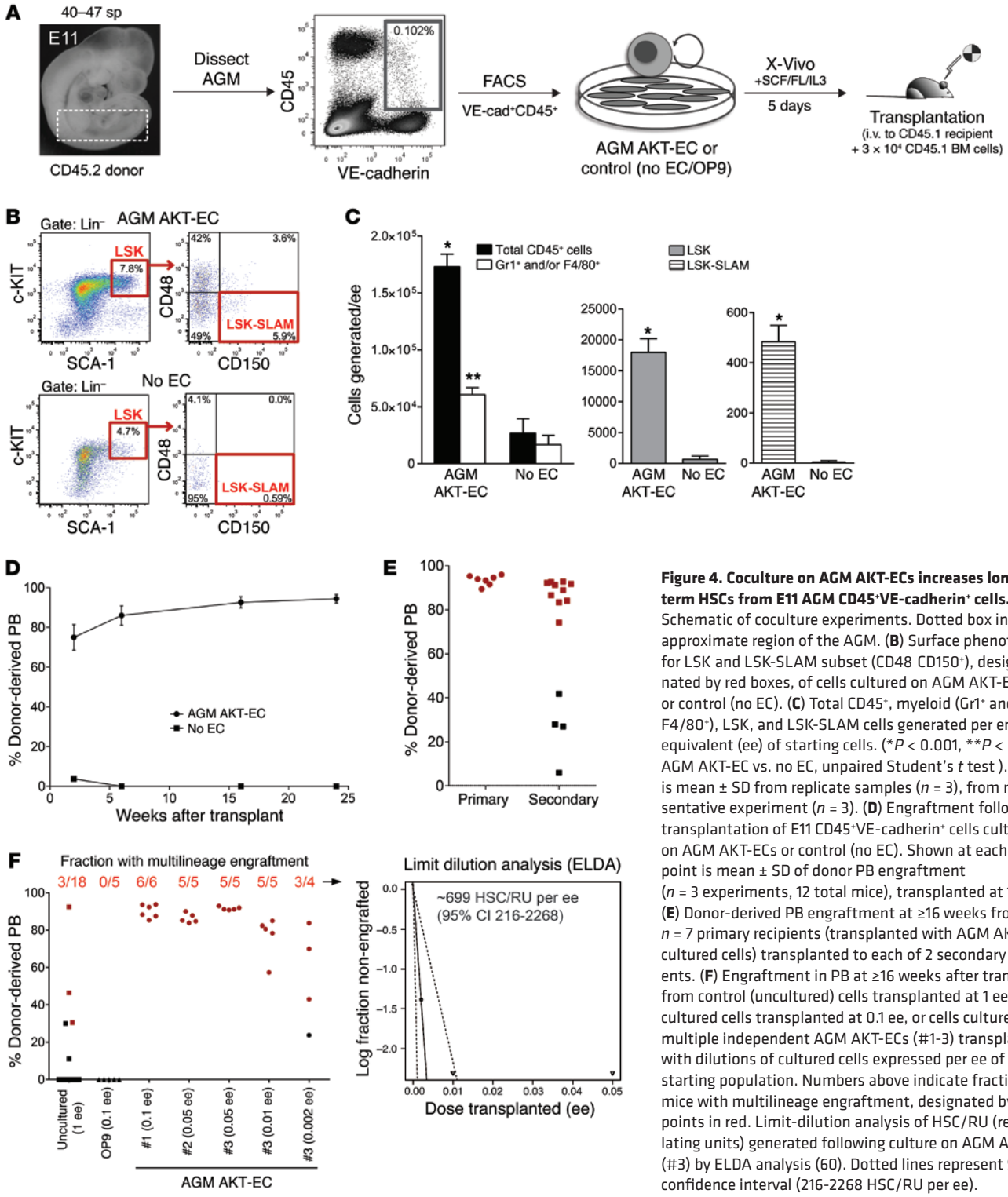

Figure 4. Coculture on AGM AKT-ECs increases long-term HSCs from E11 AGM CD45⁺VE-cadherin⁺ cells. (**A**) Schematic of coculture experiments. Dotted box indicates approximate region of the AGM. (**B**) Surface phenotyping for LSK and LSK-SLAM subset ($CD48^-CD150^+$), designated by red boxes, of cells cultured on AGM AKT-ECs or control (no EC). (**C**) Total $CD45^+$, myeloid ($Gr1^+$ and/or $F4/80^+$), LSK, and LSK-SLAM cells generated per embryo equivalent (ee) of starting cells. (*$P < 0.001$, **$P < 0.01$, AGM AKT-EC vs. no EC, unpaired Student's *t* test). Shown is mean ± SD from replicate samples ($n = 3$), from representative experiment ($n = 3$). (**D**) Engraftment following transplantation of E11 $CD45^+$VE-cadherin$^+$ cells cultured on AGM AKT-ECs or control (no EC). Shown at each time point is mean ± SD of donor PB engraftment ($n = 3$ experiments, 12 total mice), transplanted at 1 ee. (**E**) Donor-derived PB engraftment at ≥16 weeks from $n = 7$ primary recipients (transplanted with AGM AKT-cultured cells) transplanted to each of 2 secondary recipients. (**F**) Engraftment in PB at ≥16 weeks after transplant from control (uncultured) cells transplanted at 1 ee, OP9-cultured cells transplanted at 0.1 ee, or cells cultured on multiple independent AGM AKT-ECs (#1-3) transplanted with dilutions of cultured cells expressed per ee of starting population. Numbers above indicate fraction of mice with multilineage engraftment, designated by data points in red. Limit-dilution analysis of HSC/RU (repopulating units) generated following culture on AGM AKT-ECs (#3) by ELDA analysis (60). Dotted lines represent 95% confidence interval (216-2268 HSC/RU per ee).

1B) and found that each was capable of $CD45^+$ hematopoietic cell generation from E9.5–E10 P-Sp/AGM–derived HE (Supplemental Figure 5A). However, in contrast to AGM AKT-ECs, coculture of HE with OP9 stroma–expressing NOTCH ligands did not induce engrafting hematopoietic cells (Supplemental Figure 5B).

Altogether, these results are consistent with the known requirement for NOTCH activation during the endothelial-to-hematopoietic transition. However, whereas NOTCH ligand–expressing OP9 stromal cells can promote induction of hematopoietic activity from AGM/P-Sp HE, AGM AKT-ECs provide additional signals to promote their induction into definitive HSCs capable of high-level, multilineage engraftment in adult recipients.

AGM-derived EC coculture amplifies HSCs from E11 AGM VE-cadherin⁺CD45⁺ hematopoietic cells. Subsequent to their induction

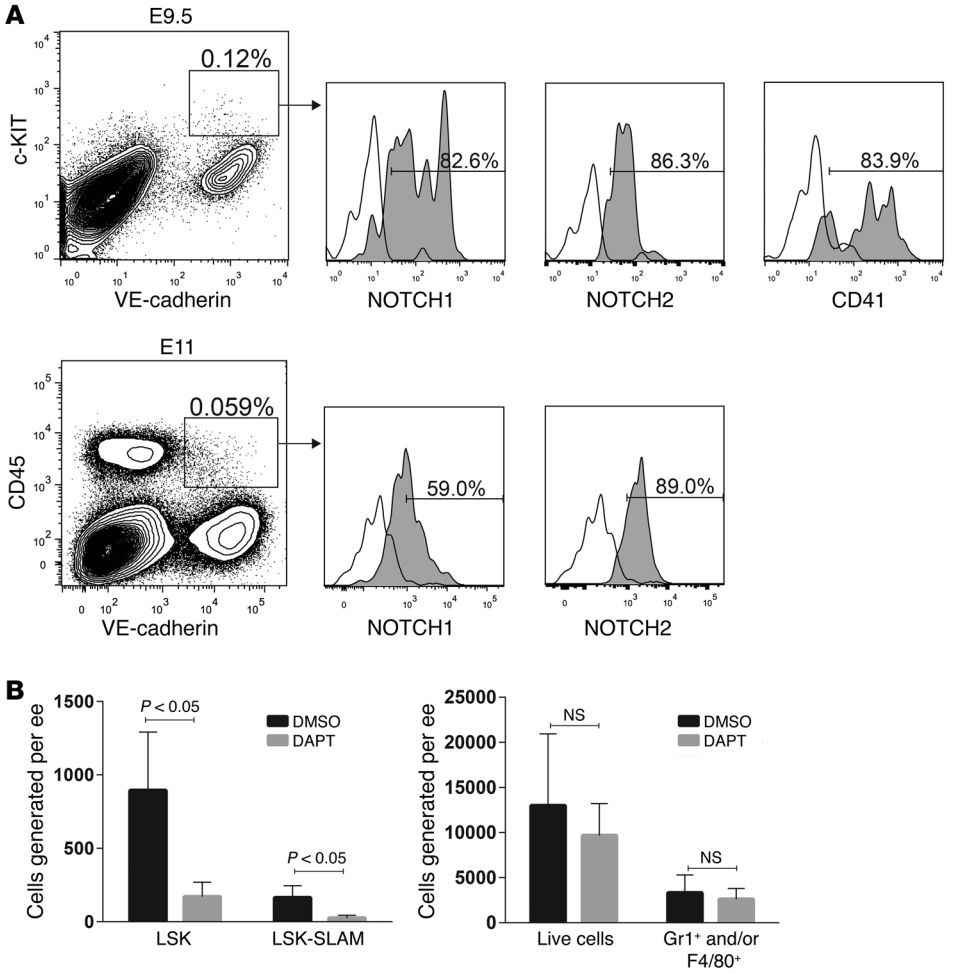

Figure 5. NOTCH pathway inhibition reduces generation of phenotypic HSCs during AGM AKT-EC coculture. (**A**) Surface expression by staining with antibodies specific for NOTCH1 and NOTCH2 on E11 VE-cadherin$^+$CD45$^+$ and E9.5 VE-cadherin$^+$c-KIT$^+$ hematopoietic progenitor cells from dissected P-Sp/AGM. (**B**) Total live cells, myeloid cells (Gr1$^+$ and/or F4/80$^+$), LSK (SCA1$^+$c-KIT$^+$Gr1$^-$F4/80$^-$) cells, and LSK-SLAM (SCA1$^+$c-KIT$^+$Gr1$^-$F4/80$^-$CD150$^+$CD48$^-$) cells generated from sorted E11.5 AGM-derived VE-cadherin$^+$CD45$^+$ cells following 5 days cultures on AGM AKT-ECs in the presence of gamma-secretase inhibitor DAPT or control (DMSO). Shown is mean ± SD of n = 3 replicate samples, from a representative experiment (n = 2).

from embryonic precursors in the P-Sp/AGM, nascent HSCs must receive signals that inhibit their lineage-specific differentiation and promote their self-renewal. To examine whether AGM AKT-ECs could support such maintenance and amplification of HSC activity from already specified hematopoietic cells, we cocultured FACS-isolated VE-cadherin$^+$CD45$^+$ cells from E11 AGM (40–47 sp with AGM AKT-ECs in X-Vivo and hematopoietic cytokines (SCF, IL3, FLT3L) (Figure 4A). E11 AGM VE-cadherin$^+$CD45$^+$ cells contain the earliest long-term engrafting HSCs that are reliably detected by standard transplantation assays into adult recipients, as well as hematopoietic cells undergoing maturation to adult-engrafting HSCs (16, 41). Following 5 days of coculture with AGM AKT-ECs, E11 AGM VE-cadherin$^+$CD45$^+$ cells generated a population of LSK stem/progenitor cells — as well as a detectable population with strict HSC phenotype, lineage$^-$SCA1$^+$c-KIT$^+$CD48$^-$CD150$^+$ (LSK-SLAM), that was mostly absent in control cultures without EC stroma (Figure 4, B and C). Since AGM-stage HSCs do not express the SLAM antigen CD150 (42), this suggested maturation of some embryonic-stage HSCs to a fetal/adult-like HSC phenotype during the culture period. Consistent with this HSC phenotype, cells cocultured with AGM AKT-ECs generated high-level, long-term, multilineage, donor-derived reconstitution (beyond 24 weeks) in the PB, BM, spleen, and thymus of transplanted adult mice (Figure 4D and Supplemental Figure 3B). Furthermore, multilineage PB engraftment was observed following transplantation into secondary recipients (Figure 4E and Supplemental Figure 3B). In contrast, no long-term engraftment was observed in mice transplanted with control (no ECs) cultured cells (Figure 4D). Whereas only a portion of mice transplanted with 1 embryo equivalent of uncultured cells were engrafted long-term, cells cultured on multiple, independently derived AGM AKT-ECs demonstrated robust multilineage engraftment when transplanted at 0.05–0.1 embryo equivalents (Figure 4F). Limit-dilution transplantation demonstrated the generation of approximately 699 HSC repopulating units (HSC/RU) per embryo equivalent of starting cells (ELDA, 95% CI 216-2268), which is comparable to the estimated number of LSK-SLAM cells detected per embryo equivalent following coculture (Figure 4, C and F). Estimates of HSC/RU within the initial VE-cadherin$^+$CD45$^+$ population at this stage from previous studies (15, 16) and our own studies (see below) demonstrate ≤1 HSC/RU per AGM. Thus, given the initial number of total VE-cadherin$^+$CD45$^+$ cells and HSC/RU detected per E11 AGM (16), the amplification of HSC/RU by AGM AKT-ECs must involve both maturation of VE-Caderhin$^+$CD45$^+$ precursors to definitive HSCs and self-renewal of HSCs once specified, consistent with similar studies of E11 AGM HSC amplification by reaggregation methods (16). Furthermore, in addition to amplification of HSCs from the VE-cadherin$^+$CD45$^+$ hematopoietic population, AGM AKT-EC culture could also induce engrafting HSCs from E11 VE-cadherin$^+$CD45$^-$ cells (Supplemental Figure 6), a population

also previously shown to contain precursors capable of maturation to HSCs following reaggregation culture (39). Altogether, these results demonstrate that AGM AKT-ECs provide an in vitro niche capable of supporting a robust increase of phenotypic and functional HSC activity from E11 embryo AGM VE-Caderhin$^+$CD45$^+$ hematopoietic cells, consistent with a role in promoting further HSC maturation, maintenance, and self-renewal following hematopoietic induction from HE.

NOTCH activation promotes amplification of HSCs from E11 AGM-derived VE-cadherin$^+$CD45$^+$ hematopoietic cells. NOTCH1 is expressed in the emerging hematopoietic clusters in the P-Sp/AGM (31) and is required for initial HSC generation (26, 27). We have shown that induction of hematopoeitic cells from E9.5 AGM/P-Sp-derived HE can be blocked by preventing NOTCH pathway activation with gamma-secretase inhibitor treatment during AGM AKT-EC coculture (Figure 3E). We observed surface expression of NOTCH1, as well as NOTCH2, in specified AGM hematopoietic progenitors (expressing hematopoietic surface markers: E9.5 c-KIT and CD41; E11 CD45) (Figure 5A). Importantly, NOTCH1 and NOTCH2 surface expression in nascent AGM hematopoietic cells suggests that, following the initial requirement for NOTCH1 in hematopoietic induction in the AGM/P-Sp, HSCs may continue to be receptive to NOTCH pathway activation mediated by ligand-expressing ECs. To test whether AGM-derived HSCs require the NOTCH pathway during the phase of expansion in AGM AKT-EC coculture, we cultured E11 VE-cadherin$^+$CD45$^+$ cells on AGM AKT-ECs with gamma-secretase inhibitor DAPT. We observed significantly reduced LSK and LSK-SLAM cell numbers, but not total or myeloid cell numbers, in cultures with DAPT compared with control (DMSO-treated) cultures (Figure 5B), suggesting a specific effect on hematopoietic stem/progenitor cells at this stage.

Based on these findings, we then tested whether activation of NOTCH signaling by immobilized ligand was sufficient to amplify long-term HSCs from E11 AGM-derived VE-cadherin$^+$CD45$^+$ cells in the absence of EC stroma. To activate NOTCH signaling, we employed Delta1 (Delta1$^{ext\text{-}IgG}$), consisting of the extracellular domain of human Delta1 fused to the Fc domain of human IgG1 (hIgG1) (43, 44). We have previously shown that culture of murine adult BM HSCs with immobilized Delta1$^{ext\text{-}IgG}$ and hematopoietic cytokines inhibits myeloid differentiation in vitro and generates increased numbers of LSK multipotent progenitors capable of short-term, multilineage engraftment (44). We here cultured E11 AGM-derived VE-cadherin$^+$CD45$^+$ cells on Delta1$^{ext\text{-}IgG}$ or control hIgG, in media containing FBS and hematopoietic cytokines SCF, FLT3L, IL-6, and TPO (4GF) (Figure 6A). Based on previously reported studies suggesting an inhibitory effect of the TGF-β pathway during AGM-stage hematopoiesis (45), we found that the addition of a small molecule TGF-β inhibitor (SB431542 or LY364947) was essential in order to generate outgrowth of LSK cells (Supplemental Figure 7). E11 VE-cadherin$^+$CD45$^+$ AGM-derived cells cultured with hematopoietic cytokines and TGF-β inhibitor SB431542 (4GF+SB) on either Delta1$^{ext\text{-}IgG}$ or hIgG, were mostly VE-cadherin$^-$ after 5 days, consistent with phenotypic maturation from the AGM to later developmental stages of hematopoiesis where VE-cadherin expression is lost (ref. 41 and Figure 6B). Neither hIgG- nor Delta1$^{ext\text{-}IgG}$-cultured cells displayed notable erythroid, B cell, T cell, or NK cell marker expression at day 5 (data not shown). Delta1$^{ext\text{-}IgG}$ cultured cells generated significantly higher LSK cell numbers compared with hIgG-cultured cells, which produced mostly F4/80$^+$ and/or Gr1$^+$ myeloid cells (Figure 6, B and C). Delta1$^{ext\text{-}IgG}$-cultured cells also generated significantly increased myeloid, erythroid, and mixed lineage colony-forming progenitors compared with the uncultured starting-cell population or cells cultured on control hIgG (Figure 6D). Prolonged culture on Delta1$^{ext\text{-}IgG}$, but not hIgG, generated increasing populations of CD25$^+$ and CD25$^+$Thy1.2$^+$ cells (Figure 6E), consistent with a known role of NOTCH1 activation in promoting early T cell differentiation (46). However, cells cultured 5 days on Delta1$^{ext\text{-}IgG}$-maintained both B-lymphoid (CD19$^+$B220$^+$) and T-lymphoid (CD4$^+$CD8$^+$) differentiation capacity in secondary OP9 or OP9-DL1 stromal cell cultures, whereas control cultured cells demonstrated no T-lymphoid capacity (Figure 6F). Together, these results demonstrate that in vitro activation of NOTCH pathway by Delta1$^{ext\text{-}IgG}$ in AGM-derived VE-cadherin$^+$CD45$^+$ hematopoietic cells promotes expansion of phenotypic and functional hematopoietic stem/progenitor populations with multilineage hematopoietic activity.

We next sought to determine whether cells generated on NOTCH ligand from AGM-derived hematopoietic cells were also capable of short- and long-term multilineage engraftment in vivo. E11 VE-cadherin$^+$CD45$^+$ AGM cells cultured 5 days on Delta1$^{ext\text{-}IgG}$ or control hIgG, with 4GF+SB, were transplanted at one embryo equivalent of starting cells into lethally irradiated congenic-strain adult mice together with a small dose of congenic BM cells. For some experiments, freshly sorted CD45$^+$VE-cadherin$^+$ cells, uncultured, were also transplanted at 1 embryo equivalent per mouse to measure engraftment of the starting population. Delta1$^{ext\text{-}IgG}$-cultured E11 AGM cells demonstrated significantly increased levels of rapid donor PB engraftment (2 weeks after transplant) compared with an equivalent population of hIgG-cultured cells or cells transplanted without culture, including both the B-lymphoid (CD19) and myeloid (Gr1 and/or F4/80) compartments (Supplemental Figure 8). Furthermore, long-term multilineage engraftment was observed in mice transplanted with Delta1$^{ext\text{-}IgG}$-cultured cells, but not hIgG-cultured cells, beyond 24 weeks after transplant (Figure 6G), and multilineage engraftment was observed in secondary transplantation from primary recipients of Delta1$^{ext\text{-}IgG}$-cultured cells (Figure 6H and Supplemental Figure 3). Pooled transplantation experiments showed a significant increase in the mean donor chimerism and in the percentage of multilineage-engrafted mice long-term (>24 weeks) transplanted with Delta1$^{ext\text{-}IgG}$-cultured cells relative to mice transplanted with an equivalent dose (1 embryo) of VE-cadherin$^+$CD45$^+$ AGM-derived cells without culture (uncultured); this suggests that Delta1$^{ext\text{-}IgG}$ induced an increase in HSC numbers (Figure 6I). To quantify this effect, transplantation of freshly sorted, uncultured cells was compared with Delta1$^{ext\text{-}IgG}$-cultured cells with limiting dilutions based on fractions of the starting cell population expressed per embryo equivalent. The frequency of HSC/RU per embryo equivalent was increased greater than 8-fold in Delta1$^{ext\text{-}IgG}$-cultured cells compared with the starting population of uncultured cells (Figure 6J). Altogether, these studies suggest that defined EC-free conditions utilizing NOTCH activation by immobilized ligands is sufficient to amplify AGM-stage HSCs from specified VE-cadherin$^+$CD45$^+$ hematopoietic cells.

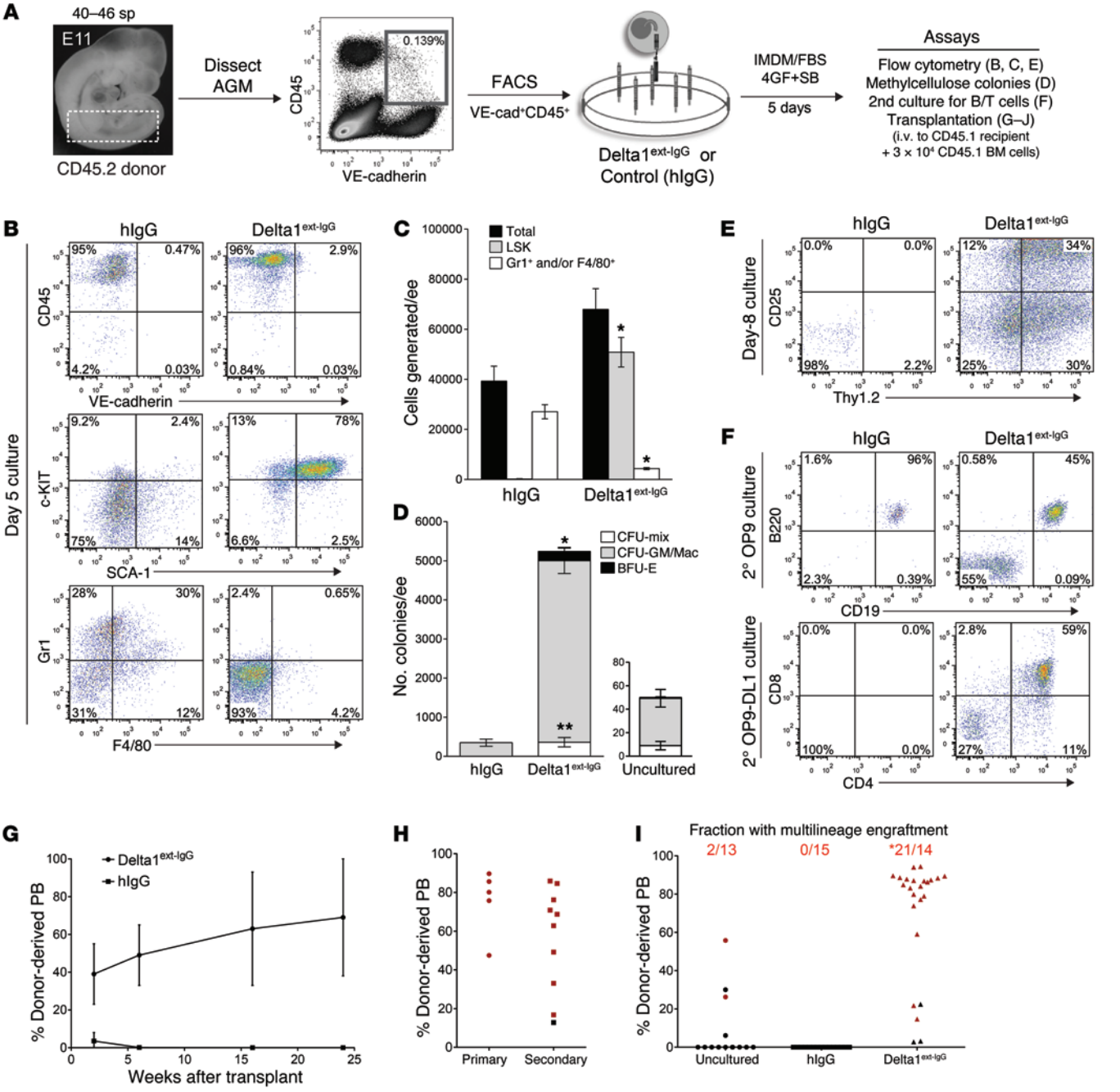

Figure 6. Delta1$^{ext\text{-}IgG}$ increases multilineage progenitors and long-term HSCs from E11 AGM-derived CD45$^+$VE-cadherin$^+$ cells. (**A**) Schematic of experimental design. Dotted box indicates approximate region of the AGM. (**B**) Phenotyping of cells cultured on Delta1$^{ext\text{-}IgG}$ or control (hIgG). (**C**) Total, LSK (SCA1$^+$c-KIT$^+$Gr1$^-$F4/80$^-$), and myeloid (Gr1$^+$ and/or F4/80$^+$) cells generated on Delta1$^{ext\text{-}IgG}$ or hIgG per embryo equivalent (ee) starting cells. (*P < 0.001, Delta$^{ext\text{-}IgG}$ vs. hIgG, unpaired Student's t test). Shown is mean ± SD (n = 3), from representative experiment (n > 3). (**D**) CFU progenitors from cells cultured on Delta1$^{ext\text{-}IgG}$ or hIgG. Shown is mean ± SD (n = 3), from representative experiment (n = 3). (*P < 0.0001 for total, **P < 0.01 for CFU-Mix, Delta$^{ext\text{-}IgG}$ vs. hIgG or uncultured, unpaired Student's t test) (**E**) T cell precursor phenotyping following extended culture (8 days) on Delta1$^{ext\text{-}IgG}$ or hIgG. (**F**) Generation of B cells (CD19$^+$B220$^+$) and T cells (CD4$^+$CD8$^+$) after culture on Delta1$^{ext\text{-}IgG}$ or hIgG followed by secondary culture on OP9/OP9-DL1. (**G**) Engraftment of cells cultured on Delta1$^{ext\text{-}IgG}$ or hIgG. Shown at each time point is mean ± SD of donor PB engraftment (n = 4 experiments, 37 total mice). (**H**) PB engraftment at ≥16 weeks from n = 5 primary recipients transplanted to each of 2 secondary recipients. (**I**) Engraftment at ≥24 weeks in mice transplanted with freshly sorted cells (uncultured), or cells cultured on Delta1$^{ext\text{-}IgG}$ or hIgG, transplanted at 1 ee. Shown above is a fraction of mice with multilineage engraftment, designated by data points in red. (*P < 0.0001, Delta1$^{ext\text{-}IgG}$ vs. uncultured, 2-sided Fisher's exact test). (**J**) Limit-dilution analysis of HSC repopulating units (HSC/RU) of cells transplanted prior to culture (uncultured) or following Delta1$^{ext\text{-}IgG}$ culture. Dotted lines represent 95% confidence interval (P = 0.00005, ELDA) (60).

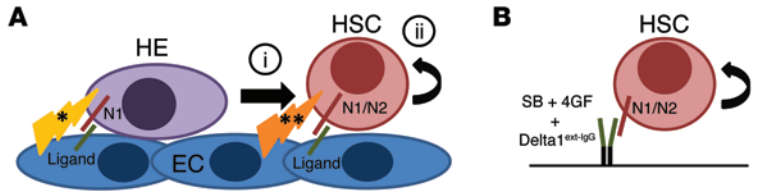

Figure 7. Model for vascular niche induction and NOTCH-mediated expansion of HSCs. (**A**) The AGM AKT-EC vascular niche promotes (i) induction of HSCs from embryonic HE, which is dependent on NOTCH activation mediated by one or more NOTCH ligands expressed on ECs to promote the endothelial-to-hematopoietic transition, as well as other EC-derived niche factors (*) to promote the generation of engrafting HSCs. (ii) Subsequent to HSC specification, further amplification of AGM-derived HSC numbers continues to involve both ligand-mediated NOTCH activation and additional EC-niche factors (**), which contribute to HSC maturation and self-renewal. (**B**) NOTCH activation by immobilized NOTCH ligand Delta1$^{ext\text{-}IgG}$, combined with hematopoietic growth factors (SCF, TPO, IL6, FLT3L) and small molecule inhibition of the TGF-β pathway (SB+4GF), is sufficient to amplify AGM-derived HSC numbers in vitro in the absence of AGM AKT-EC stroma.

Discussion

Here, we examined the capacity of the vascular niche to support embryonic HSC genesis, a complex process with developmentally unique requirements to promote both the specification of engrafting HSCs from nonengrafting precursors and subsequent self-renewal of the nascent, embryonic HSCs. We demonstrate that ECs from the AGM region are able to support robust and reproducible in vitro induction of adult-engrafting HSCs from HE and subsequently significantly expand long-term, engrafting HSC numbers dependent on NOTCH signaling (Figure 7A). We further identify conditions involving NOTCH signaling activation by immobilized ligand to amplify the nascent AGM-derived HSC population in the absence of EC stroma (Figure 7B). Importantly, these studies establish methodology to support both HSC induction and numerical expansion ex vivo from embryonic precursors, and begin to dissect critical mechanistic components of the vascular niche necessary and sufficient for this process.

Previous studies have shown that culture of whole AGM explants or reaggregated AGM stroma ex vivo can support HSC amplification from E11 embryos (15, 16, 41). Numerous stromal cell lines derived from the AGM with various properties of mesenchymal cells have been shown to support HSC maintenance in vitro, though these studies did not demonstrate the capacity of these stromal lines to promote significant numerical expansion of AGM-derived HSCs comparable to that of reaggregation culture (18, 19). Thus, the precise microenvironmental components within the AGM capable of supporting embryonic HSC expansion at this stage have remained unclear. While it is likely that multiple stromal cell types from the AGM microenvironment contribute to supporting embryonic HSCs, here we have shown that in vitro culture with AGM-derived ECs is sufficient to recapitulate robust amplification of HSCs from E11 VE-cadherin$^+$CD45$^+$ AGM hematopoietic cells. Given that limit-dilution analysis suggests approximately 1 or fewer HSCs per AGM at this stage (ref. 15 and Figure 6J), the degree of numerical expansion of HSCs in culture is consistent with previous studies of AGM reaggregation culture in which HSCs are also derived by further maturation of HSC precursors contained within the VE-cadherin$^+$CD45$^+$ population (16). However, as this rare population consists of approximately <100 cells per AGM (16, 41), this implies contribution by proliferative self-renewal of HSCs as they arise, as well, to account for the number of HSC/RU generated. Thus, the AGM AKT-EC provide signals sufficient to both mature VE-cadherin$^+$CD45$^+$ pre-HSC to definitive HSC, as well as to ensure HSC self-renewal once established.

Previous studies have also shown that, prior to E10.5 — when no high-level, adult-engrafting HSCs can be detected in the embryo — reaggregation of VE-cadherin$^+$CD41$^+$CD45$^-$ HSC precursors with OP9 stromal cells in culture at air-liquid interface can support their maturation to engrafting HSCs (39, 40), and in vitro multipotent lymphoid/myeloid hematopoietic progenitors and cells capable of engrafting conditioned newborn mice are detectable in the VE-cadherin$^+$c-KIT$^+$ population as early as E9 (36, 47). Here, we have shown that AGM/P-Sp–derived VE-cadherin$^+$ cells from embryos as early as E9, cocultured with AGM AKT-ECs, generate HSCs capable of high-level, long-term, multilineage engraftment in adult recipients. This includes the population of VE-cadherin$^+$ HPCs already expressing hematopoietic markers c-KIT and CD41. However, we also show in this study the capacity of AGM AKT-ECs to induce HSCs from HE contained within the VE-cadherin$^+$ population yet lacking expression of hematopoietic surface markers or direct clonal hematopoietic activity. Thus, we provide the first evidence, to our knowledge, that an EC niche is sufficient to recapitulate the embryonic HE-to-HSC transition ex vivo. Notably, a recent study in zebrafish suggests an essential in vivo role for a subset of somite-derived ECs in the dorsal aorta in supporting HSC induction from adjacent HE (48), further promoting the concept that ECs provide essential niche signals for HSC induction.

Importantly, further studies of the EC coculture system will facilitate the determination of paracrine signals essential for HSC generation. Since AKT activation was necessary in these studies to permit AGM-derived ECs to grow in serum-free conditions suitable for coculture with HSCs/precursors, it is impossible to rule out that some properties of AGM AKT-ECs that allow for support of HSC generation may be induced by AKT activation. In this regard, AKT activation was previously shown to be involved in HSC self-renewal in the context of the adult BM vascular niche (23), and pathways downstream of AKT-activation in ECs, including that of nitric oxide induced by fluid shear stress, have been implicated in HSC development (49–51). It is interesting to speculate that an AKT-induced nitric oxide pathway in the EC coculture system may circumvent the normal requirement for flow-mediated shear stress in HSC development, but further studies are required to investigate this possibility, as well as the potential role of other pathways downstream of AKT that may contribute to HSC generation in this system.

One pathway active in the AGM vascular niche, with an essential role in HSC genesis, is that of the NOTCH family (25). Loss-of-function studies firmly established that the NOTCH pathway is required for HSC development (26–28, 31), though recent studies suggest multiple stage-, context-, and receptor-specific functions of the NOTCH pathway in sequential processes during HSC development, including determination of arterial endothelial fate, specification of HE within lateral plate mesoderm, induction of

HSCs from HE in the dorsal aorta, and survival of HSCs in the fetal liver (32, 52–57). In addition to such roles in promoting cell fate and survival, context-specific NOTCH activation is known to regulate stem/progenitor self-renewal in some systems by inhibiting lineage-specific differentiation. In this way, NOTCH2 regulates the regeneration of multipotent progenitors and HSCs in the adult BM following injury, even though canonical NOTCH signaling may be dispensable for HSCs in adult BM during homeostasis (33, 34). Thus, ligand-mediated NOTCH activation in developing HSCs and their precursors may compose a critical component of the AGM vascular niche by limiting the differentiation of nascent HSCs as they emerge, and — in concert with other growth-factor signals — mediating their self-renewal and proliferative expansion. Consistent with this hypothesis, our studies have determined in vitro conditions whereby NOTCH activation can increase long-term engrafting HSC numbers from the newly specified E11 AGM ($CD45^+VE\text{-}cadherin^+$) hematopoietic cells. Although Delta1 was used as the ligand to activate the NOTCH pathway in these studies, multiple NOTCH ligands are expressed on AGM ECs, and our preliminary studies suggest that immobilized JAG1 and either NOTCH1 or NOTCH2 receptor–specific activation can also support AGM HSCs at this stage, though perhaps with different efficiencies (not shown). Additional studies will be required to determine whether the strength of NOTCH pathway activation mediated by differential-receptor activation may contribute in mediating self-renewal verses alternative cell fates in this regard.

Although NOTCH signaling is required during the HE-to-HSC transition, neither the use of immobilized NOTCH ligand under conditions that we showed could amplify HSCs from E11 AGM hematopoietic cells, nor the use of OP9 stroma expressing NOTCH ligands, was sufficient to induce engrafting HSC from HE. Further studies of AGM AKT-ECs may elucidate the nature of additional signals required for induction of HSCs from HE in concert with NOTCH pathway activation. We anticipate that such studies, by defining the precise signals necessary and sufficient in vitro for both specification and self-renewal of HSCs from embryonic precursors, will move us closer to the goal of bringing pluripotent stem cell technologies to therapeutic applications for HSC transplantation.

Methods

Mice. WT C57Bl6/J7 (Ly5.2/CD45.2) and congenic C57BL/6.SJL-Ly5.1-Pep3b (Ly5.1/CD45.1) mice were bred at the Fred Hutchinson Cancer Research Center. C57Bl6/J7 Ly5.2 male and female mice were used for timed matings.

Embryo dissections and cell sorting. Embryos were harvested from pregnant females, dissected free of maternal tissue, and washed extensively in PBS containing 10% FBS. Embryo age was precisely timed by counting sp. The following stages were used for studies as indicated: E9, 13–20 sp; E9.5–E10, 21–32 sp; and E11, 41–47 sp. For AGM dissections, 30-gauge needles were used to remove the caudal and rostral portions of the embryo above the forelimbs and below the hindlimbs, and subsequently to dissect off the dorsal somite tissue and ventral abdominal contents. The embryo was then splayed open lying on its dorsal surface, and remaining tissues surrounding the urogenital ridges were further dissected, leaving the intact AGM containing the dorsal aorta centrally. For embryos prior to E10, the P-Sp region was dissected by removing the rostral and caudal portions of the embryo. Dissected AGM/P-Sp tissues were pooled and treated with 0.25% collagenase (StemCell Technologies Inc.) for 25–30 minutes at 37°C, pipetted to single-cell suspension, and washed with PBS containing 10% FBS. Cells were incubated with anti–mouse CD16/CD32 (FcγRII block) and stained with the following monoclonal antibodies: FITC or APC-conjugated CD45 (clone 30-F11); FITC or APC-conjugated anti–c-KIT (clone 2B8; eBioscience); FITC-, Alexa Fluor 488-, or APC-conjugated CD41 (clone MWReg30; eBioscience); unconjugated or PE-conjugated VE-cadherin/CD144 (clone 11D4.1); or corresponding isotype controls. When staining with unconjugated CD144, following incubation with primary antibodies, cells were washed twice with PBS/FBS, and secondary staining was performed with PE-conjugated mouse anti-rat IgG2a (clone RG7/1.30). All antibodies were from BD Biosciences unless otherwise indicated. DAPI staining was used to gate out dead cells. All reagents for cell staining were diluted in PBS with FBS, and staining was carried out on ice or at 4°C. Cells were sorted on a BD FACS Aria II (BD Biosciences).

EC generation and culture. For derivation of AGM ECs, P-Sp/AGM tissues were dissected from E10–E11 embryos and sorted using VE-cadherin/CD144 (clone 11D4.1), as described previously, with APC-conjugated CD45 (clone 30-F11) — along with CD41 (clone MWReg30, eBioscience) in some experiments — to exclude hematopoietic cells. Sorted cells pooled from multiple P-Sp/AGM were cultured on 48-well tissue culture plates (>20,000 $VE\text{-}cadherin^+CD45^-$ or $VE\text{-}cadherin^+CD45^-CD41^-$ cells per well) coated with 5 μg/ml RetroNectin (r-fibronectin CH-296; Takara Bio Inc.), in media containing IMDM, 20% FBS (HyClone), Penicillin/streptomycin, L-glutamine, heparin 0.1 mg/ml (H3149-100KU; Sigma-Aldrich), endothelial mitogen 100 μg/ml (Biomedical Technologies), VEGF (50 ng/ml; PeproTech), CHIR009921 (5 μM; StemGent), and SB431542 (10 μM; R&D Systems). Following 1–2 days, colonies of ECs were infected by lentivirus with MyrAKT construct, as previously described (23). For some experiments, mock-infected ECs were also cultured in parallel, but in the absence of infection with MyrAKT, these cells did not continue to proliferate/survive after initial passage. When confluent, cells were serially split at a density of no less than 1:3 to larger wells and coated with 0.1% gelatin in above media but without added VEGF, CHIR09921, or SB431542. The first passage to T75 flask was considered passage 0, with subsequent passages every 3–4 days plated at approximately 5×10^5 cells per T75. For coculture experiments, AGM AKT-ECs at passage 15 or less were plated at a density of 4×10^4 cells per 24-well or 1×10^5 cells per 12-well the day prior. Cell populations from E9–E11 P-Sp/AGM sorted as described were plated on AGM AKT-ECs, or control conditions (no ECs or OP9 cells), in serum-free media consisting of X-Vivo 20 (Lonza) with recombinant cytokines (PeproTech): stem cell factor (SCF), FLT3 ligand (FL), interleukin-3 (IL-3) — each at 100 ng/ml — and thrombopoietin (TPO) at 20 ng/ml, as indicated. Sorted cells were cocultured at a density of approximately 1–2 embryo equivalents per 24-well or 3–5 per 12-well. Cells sorted per embryo equivalent varied based on embryonic stage and the population sorted (ranges: E9–E10 total $VE\text{-}cadherin^+$: 1750–6961; E9–E10 $VE\text{-}cadherin^+c\text{-}KIT^-$ and/or $CD41^-CD45^-$ HE: 1600–6408; E9.5–E10 $VE\text{-}cadherin^+c\text{-}KIT^+$: 210–581; E11 $VE\text{-}cadherin^+CD45^+$: 38–619). For indicated experiments, DAPT (in DMSO, final concentration 5 μM; EMD Millipore) or equivalent volume DMSO was added as indicated. In some experiments, AGM AKT-ECs were cultured alone with serum-

free media and hematopoietic cytokines, and analyzed in parallel with coculture experiments for phenotypic hematopoietic cells, CFU, and engraftment following transplantation, to rule out hematopoietic contribution from AKT-ECs.

Culture on NOTCH ligands. Delta1$^{ext\text{-}IgG}$ was generated as previously described (43). Nontissue culture-treated plates (Falcon; BD Biosciences) were incubated with Delta1$^{ext\text{-}IgG}$ (dose range from 0.5 μg/ml–20 μg/ml), or hIgG1 (Sigma-Aldrich) diluted in PBS together with 5 μg/ml RetroNectin (r-fibronectin CH-296; Takara Bio Inc.), incubated overnight at 4°C. Wells were washed extensively with PBS prior to adding media. Media consisted of either Iscove's Modified Dulbeco's Media (IMDM) (Invitrogen) containing 20% FBS (HyClone), supplemented with Penicillin/Streptomycin (Sigma-Aldrich), small molecule inhibitor of TGFβ pathway (10 μM; SB431541, Tocris Bioscience, or LY364947, R&D Systems; added 1:1,000 from stock 10-mM solution in DMSO), and recombinant hematopoietic cytokines (PeproTech): SCF, FL, interleukin-6 (IL-6) at 100 ng/ml, and TPO at 20 ng/ml; some initial experiments also included recombinant interleukin-11 (IL-11) at 10 ng/ml and IL-3 at 100 ng/ml, though these cytokines were excluded in later experiments, as they did not improve engraftment of cultured cells. For experiments examining the effect of TGF-β1, cells were cultured in above media or serum-free (StemSpan; StemCell Technologies Inc.) with above cytokines and recombinant TGF-β1 (1 or 10 ng/ml; R&D systems) added as indicated. Freshly sorted VE-cadherin$^+$CD45$^+$ cells from dissected E11 embryos were resuspended in media with cytokines and added to coated 96-well plates (approximately 2–5 embryo equivalent of cells per 96-well). Cells were passaged to larger wells prepared as described once cells were nearly confluent, when necessary. For most experiments, cells were harvested for phenotypic analysis, CFU, or transplantation assays at day 5 of culture, unless otherwise indicated. For experiments involving transplants from E11 VE-cadherin$^+$CD45$^+$ cells, only AGM from early E11–E11.5 (40–46 somite range) were included, since HSC frequency increases in the late E11 AGM (58). Preliminary experiments optimizing Delta1$^{ext\text{-}IgG}$ ligand concentration showed a trend toward improved engraftment with relatively lower doses of Delta1$^{ext\text{-}IgG}$ (0.5–2.5 μg/ml) (not shown), so these concentrations were used for subsequent analysis.

Hematopoietic assays on secondary OP9 stromal culture. OP9 cells and OP9 cells expressing DLL1 (OP9-DL1) or DLL4 (OP9-DL4), a gift of J.C. Zuniga-Pflucker (University of Toronto, Toronto, Ontario, Canada), were cultured as previously described (59). For lymphocyte assays, cells harvested following culture were replated onto OP9 or OP9-DL1 in OP9 media (αMEM, FBS 20%, penicillin/streptomycin) containing recombinant FLT3-L (FL, 10 ng/ml) and IL-7 (1 ng/ml). Cells were replated at 7-day intervals, or when confluent to fresh OP9 layers, and analyzed by flow cytometry at 7-day intervals for T cell (CD44, CD25, CD4, CD8), and B cell (CD19, B220) markers, using antibodies indicated below.

Cell surface analysis. Cells were harvested from freshly isolated P-Sp/AGM as described previously or pipetted from tissue-culture wells and washed with PBS with 2% FBS. Cells were preincubated with anti–mouse CD16/CD32 (FcγRII block) and then stained with various combinations of the following monoclonal antibodies for cell-surface analysis: APC- or FITC-conjugated CD45 (clone 30-F11); APC-, Alexa Fluor 488–, or FITC-conjugated CD41 (clone MWReg30; eBioscience); purified or PE-conjugated VE-cadherin/CD144 (clone 11D4.1); FITC-, PE-, or PECy7-conjugated anti-SCA1 (anti–Ly-6A/E, clone E13-161.7); APC- or APCeFluor780-conjugated anti–c-KIT (clone 2B8; eBioscience); PECy7-conjugated anti-Thy1.2 (clone 53-2.1); APCeFluor780-conjugated anti-F4/80; APC-Cy7–, PE-, or APC-conjugated anti-CD19 (clone ID3); PerCP- or APCeFluor780-conjugated Gr-1 (anti–Ly6-G, clone RB6-8C5; eBioscience); PerCP-, APCeFluor780-, or FITC-conjugated anti-B220/CD45R (clone RA3-6B2; eBioscience); PE- or APC-Cy7–conjugated anti-CD25 (clone PC61); APC-conjugated CD44 (clone IM7); FITC- or PE-conjugated CD4 (clone RM4-5); FITC- or PerCP-conjugated CD8 (clone 53-6.7); PE-conjugated anti–VE-cadherin/CD144 (clone 16B1; eBioscience); APC- or APC-Cy7–conjugated FLK-1 (clone Avas 12a1); FITC-, PE-, APCeFluor780-, or PE-Cy5–conjugated TER-119 (Ly76, clone TER-119; eBioscience); FITC-conjugated anti-NK1.1 (clone PK136; eBioscience); PE- or PerCP/C5.Cy5-conjugated CD150 (clone TC15-12F12.2; Biolegend); PeCy7-conjugated CD48 (clone HM48-1); APC-conjugated anti-NOTCH1 (clone HMN1-12; Biolegend); NOTCH2 (clone HMN2-35; BioLegend); DLL1 (clone HMD1-3; Biolegend) or DLL4 (clone HMD4-1; Biolegend); APC- or PE-conjugated JAG1 (clone HMJ1-29; Biolegend/eBioscience); eFluor 660–conjugated JAG2 (clone HMJ2-1; eBioscience); or corresponding isotype control antibodies. For analysis involving unconjugated VE-cadherin antibody (clone 11D4.1), following incubation with primary antibodies, cells were washed twice with PBS/2% FBS, and secondary staining was performed with PE-conjugated mouse anti–rat IgG2a (clone RG7/1.30). AGM AKT-ECs were excluded from analysis of cocultured cells by gating based on expression of VE-cadherin or FLK-1. Based on the lineage markers expressed in cells following coculture experiments, lineage-negative cells were gated by exclusion of Gr-1, F4/80, TER119, and B220 expression, unless otherwise indicated. DAPI was used to exclude dead cells. Flow cytometry was performed on a BD FACSCanto II (BD Biosciences) and data analyzed using FlowJo Software. Specificity of NOTCH1 and NOTCH2 antibodies was confirmed by comparing expression on WT and NOTCH1-deficient embryonic stem cells, and WT or NOTCH2-deficient hematopoietic cells from mice with inducible deletion of *Notch2* (not shown).

CFU progenitor analysis. Freshly sorted AGM/PsP cells or cultured cells pipetted from wells were washed and counted, resuspended in IMDM, added to M3434 methylcellulose semi-solid media containing hematopoietic cytokines (StemCell Technologies Inc.), and plated in triplicate 30mm petri dishes. After 7 days of culture, individual colonies were counted and scored by morphology as myeloid (CFU-GM, granulocyte/monocyte; or CFU-Mac, macrophage), erythroid (burst-forming unit-erythroid, BFU-E), or mixed lineage (CFU-mix, containing both erythroid and myeloid cells). For most analysis, numbers of each CFU type are enumerated per 1 embryo equivalent of starting cells prior to culture.

Transplantation assays. Freshly sorted Ly5.2/CD45.2 AGM cells or cultured cells harvested by gentle pipetting off of wells were washed with PBS with 2% FBS and resuspended in 100 μl PBS/2% FBS per mouse transplanted. Freshly harvested Ly5.1/CD45.1 BM cells were added at 3×10^4 cells in 100 μl PBS/FBS per mouse to provide hematopoietic rescue. Cells were co-injected into lethally irradiated (900–1,000 cGy using a Cesium source) Ly5.1/CD45.1 adult recipients via the tail vein. For secondary transplants, 10^6 whole BM cells harvested from primary recipients were transplanted to lethally irradiated Ly5.1/CD45.1 recipients via the tail vein. FACS analysis of PB obtained by retro-orbital bleeds was performed at indicated intervals — and from

cells obtained from harvested BM, spleen, and thymic tissues at the time of the secondary transplant — at least 16 weeks following the primary transplant. Staining for donor Ly5.2/CD45.2 with APC-eFluor780– or PE-Cy7–conjugated CD45.2 (clone 104; eBioscience) was distinguished from Ly5.1/CD45.1 (recipient/rescue cells) stained with PE-Cy7 or eFlour-450–conjugated CD45.1 (clone A20; eBioscience) and myeloid and T/B lymphoid lineage determination was obtained by costaining with the monoclonal antibodies: FITC-conjugated anti-CD3 (clone 17A2); PE-conjugated F4/80 (clone BM8; eBioscience); APC-conjugated anti-CD19 (clone ID3); PerCP-conjugated GR-1 (anti–Ly6-G, clone RB6-8C5); PE-conjugated CD8 (clone 53-6.7); and PECy5-conjugated CD4 (clone RM4-5). Multilineage engraftment was defined as >5% donor (CD45.2) contribution to the PB with each of donor myeloid (Gr-1 and/or F4/80), B cell (CD19), and T cell (CD3) engraftment detected at ≥0.5% of total PB.

Statistics. For statistical analysis, 2-tailed, unpaired Student's *t* test was used to calculate *P* values unless otherwise indicated. *P* value <0.05 was considered significant. ELDA software (http://bioinf.wehi.edu.au/software/elda/) (60) was used for limit-dilution transplantation analysis, calculated using the fraction of mice engrafted at each dilution of starting cells expressed per embryo equivalent, where engraftment was defined as >5% donor (CD45.2) contribution to the PB, with each of donor myeloid (Gr-1 and/or F4/80), B cell (CD19), and T cell (CD3) engraftment detected at least 0.5% of total PB at 20 weeks after transplant.

Study approval. All animal studies were conducted in accordance with the NIH guidelines for humane treatment of animals and were approved by the Institutional Animal Care and Use Committee at the Fred Hutchinson Cancer Research Center.

Acknowledgments

We thank Cynthia Nourigat, David A. Flowers, Stacey Dozono, and LaKeisha Perkins for their technical assistance. This work was supported by the NIH NHLBI UO1 grant HL100395 and Ancillary Collaborative Grant HL099997. B.K. Hadland is supported by the Alex's Lemonade Stand Foundation, the NIH under NCI Paul Calabresi Career Development Award K12CA076930, and previously by the Ruth L. Kirschstein National Research Service Award T32CA009351. The authors have no conflicting financial interests.

Address correspondence to: Irwin Bernstein, Clinical Research Division, Fred Hutchinson Cancer Research Center, 1100 Fairview Ave. N., D2-373, Seattle, Washington 98109, USA. Phone: 206.667.4886; E-mail: ibernste@fhcrc.org.

1. Dzierzak E, Speck NA. Of lineage and legacy: the development of mammalian hematopoietic stem cells. *Nat Immunol*. 2008;9(2):129–136.
2. Frame JM, McGrath KE, Palis J. Erythro-myeloid progenitors: "Definitive" hematopoiesis in the conceptus prior to the emergence of hematopoietic stem cells. *Blood Cells Mol Dis*. 2013;51(4):220–225.
3. Lin Y, Yoder MC, Yoshimoto M. Lymphoid progenitor emergence in the murine embryo and yolk sac precedes stem cell detection. *Stem Cells Dev*. 2014;23(11):1168–1177.
4. Medvinsky A, Rybtsov S, Taoudi S. Embryonic origin of the adult hematopoietic system: advances and questions. *Development*. 2011;138(6):1017–1031.
5. Muller AM, Medvinsky A, Strouboulis J, Grosveld F, Dzierzak E. Development of hematopoietic stem cell activity in the mouse embryo. *Immunity*. 1994;1(4):291–301.
6. Ema H, Nakauchi H. Expansion of hematopoietic stem cells in the developing liver of a mouse embryo. *Blood*. 2000;95(7):2284–2288.
7. Kieusseian A, Brunet de la Grange P, Burlen-Defranoux O, Godin I, Cumano A. Immature hematopoietic stem cells undergo maturation in the fetal liver. *Development*. 2012;139(19):3521–3530.
8. Gordon-Keylock S, Sobiesiak M, Rybtsov S, Moore K, Medvinsky A. Mouse extraembryonic arterial vessels harbor precursors capable of maturing into definitive HSCs. *Blood*. 2013;122(14):2338–2345.
9. Swiers G, Rode C, Azzoni E, de Bruijn MF. A short history of hemogenic endothelium. *Blood Cells Mol Dis*. 2013;51(4):206–212.
10. North T, et al. Cbfa2 is required for the formation of intra-aortic hematopoietic clusters. *Development*. 1999;126(11):2563–2575.
11. Swiers G, et al. Early dynamic fate changes in haemogenic endothelium characterized at the single-cell level. *Nat Commun*. 2013;4:2924.
12. Boisset JC, van Cappellen W, Andrieu-Soler C, Galjart N, Dzierzak E, Robin C. In vivo imaging of haematopoietic cells emerging from the mouse aortic endothelium. *Nature*. 2010;464(7285):116–120.
13. Swiers G, Speck NA, de Bruijn MF. Visualizing blood cell emergence from aortic endothelium. *Cell Stem Cell*. 2010;6(4):289–290.
14. Yokomizo T, Dzierzak E. Three-dimensional cartography of hematopoietic clusters in the vasculature of whole mouse embryos. *Development*. 2010;137(21):3651–3661.
15. Kumaravelu P, et al. Quantitative developmental anatomy of definitive haematopoietic stem cells/long-term repopulating units (HSC/RUs): role of the aorta-gonad-mesonephros (AGM) region and the yolk sac in colonisation of the mouse embryonic liver. *Development*. 2002;129(21):4891–4899.
16. Taoudi S, et al. Extensive hematopoietic stem cell generation in the AGM region via maturation of VE-cadherin$^+$CD45$^+$ pre-definitive HSCs. *Cell Stem Cell*. 2008;3(1):99–108.
17. Li W, et al. Primary endothelial cells isolated from the yolk sac and para-aortic splanchnopleura support the expansion of adult marrow stem cells in vitro. *Blood*. 2003;102(13):4345–4353.
18. Ohneda O, et al. Hematopoietic stem cell maintenance and differentiation are supported by embryonic aorta-gonad-mesonephros region-derived endothelium. *Blood*. 1998;92(3):908–919.
19. Oostendorp RA, et al. Stromal cell lines from mouse aorta-gonads-mesonephros subregions are potent supporters of hematopoietic stem cell activity. *Blood*. 2002;99(4):1183–1189.
20. Xu MJ, et al. Stimulation of mouse and human primitive hematopoiesis by murine embryonic aorta-gonad-mesonephros-derived stromal cell lines. *Blood*. 1998;92(6):2032–2040.
21. Butler JM, et al. Endothelial cells are essential for the self-renewal and repopulation of NOTCH-dependent hematopoietic stem cells. *Cell Stem Cell*. 2010;6(3):251–264.
22. Chute JP, et al. Ex vivo culture with human brain endothelial cells increases the SCID-repopulating capacity of adult human bone marrow. *Blood*. 2002;100(13):4433–4439.
23. Kobayashi H, et al. Angiocrine factors from AKT-activated endothelial cells balance self-renewal and differentiation of haematopoietic stem cells. *Nat Cell Biol*. 2010;12(11):1046–1056.
24. Poulos MG, et al. Endothelial jagged-1 is necessary for homeostatic and regenerative hematopoiesis. *Cell reports*. 2013;4(5):1022–1034.
25. Bigas A, Espinosa L. Hematopoietic stem cells: to be or NOTCH to be. *Blood*. 2012;119(14):3226–3235.
26. Kumano K, et al. NOTCH1 but not NOTCH2 is essential for generating hematopoietic stem cells from endothelial cells. *Immunity*. 2003;18(5):699–711.
27. Hadland BK, et al. A requirement for NOTCH1 distinguishes 2 phases of definitive hematopoiesis during development. *Blood*. 2004;104(10):3097–3105.
28. Guiu J, et al. Hes repressors are essential regulators of hematopoietic stem cell development downstream of NOTCH signaling. *J Exp Med*. 2013;210(1):71–84.
29. Kim PG, et al. Signaling axis involving Hedgehog, NOTCH, and Scl promotes the embryonic endothelial-to-hematopoietic transition. *Proc Natl Acad Sci U S A*. 2013;110(2):E141–E150.
30. Nakagawa M, et al. AML1/RUNX1 rescues NOTCH1-null mutation-induced deficiency of para-aortic splanchnopleural hematopoiesis. *Blood*. 2006;108(10):3329–3334.
31. Robert-Moreno A, Espinosa L, de la Pompa JL, Bigas A. RBPjκ-dependent NOTCH function regulates GATA2 and is essential for the formation of intra-embryonic hematopoietic cells. *Develop-*

ment. 2005;132(5):1117–1126.
32. Gerhardt DM, et al. The NOTCH1 transcriptional activation domain is required for development and reveals a novel role for NOTCH1 signaling in fetal hematopoietic stem cells. *Genes Dev*. 2014;28(6):576–593.
33. Maillard I, et al. Canonical notch signaling is dispensable for the maintenance of adult hematopoietic stem cells. *Cell Stem Cell*. 2008;2(4):356–366.
34. Varnum-Finney B, Halasz LM, Sun M, Gridley T, Radtke F, Bernstein ID. NOTCH2 governs the rate of generation of mouse long- and short-term repopulating stem cells. *J Clin Invest*. 2011;121(3):1207–1216.
35. Butler JM, Rafii S. Generation of a vascular niche for studying stem cell homeostasis. *Methods Mol Biol*. 2012;904:221–233.
36. Yoder MC, Hiatt K, Dutt P, Mukherjee P, Bodine DM, Orlic D. Characterization of definitive lymphohematopoietic stem cells in the day 9 murine yolk sac. *Immunity*. 1997;7(3):335–344.
37. Fraser ST, Ogawa M, Yu RT, Nishikawa S, Yoder MC. Definitive hematopoietic commitment within the embryonic vascular endothelial-cadherin(+) population. *Exp Hematol*. 2002;30(9):1070–1078.
38. Nakano T, Kodama H, Honjo T. Generation of lymphohematopoietic cells from embryonic stem cells in culture. *Science*. 1994;265(5175):1098–1101.
39. Rybtsov S, et al. Hierarchical organization and early hematopoietic specification of the developing HSC lineage in the AGM region. *J Exp Med*. 2011;208(6):1305–1315.
40. Rybtsov S, et al. Tracing the origin of the HSC hierarchy reveals an SCF-dependent, IL-3-independent CD43(-) embryonic precursor. *Stem Cell Reports*. 2014;3(3):489–501.
41. Taoudi S, Morrison AM, Inoue H, Gribi R, Ure J, Medvinsky A. Progressive divergence of definitive haematopoietic stem cells from the endothelial compartment does not depend on contact with the foetal liver. *Development*. 2005;132(18):4179–4191.
42. McKinney-Freeman SL, et al. Surface antigen phenotypes of hematopoietic stem cells from embryos and murine embryonic stem cells. *Blood*. 2009;114(2):268–278.
43. Varnum-Finney B, et al. Immobilization of NOTCH ligand, Delta-1, is required for induction of notch signaling. *J Cell Sci*. 2000; 113(pt 23):4313–4318.
44. Varnum-Finney B, Brashem-Stein C, Bernstein ID. Combined effects of NOTCH signaling and cytokines induce a multiple log increase in precursors with lymphoid and myeloid reconstituting ability. *Blood*. 2003;101(5):1784–1789.
45. Sato T, et al. Evi-1 promotes para-aortic splanchnopleural hematopoiesis through up-regulation of GATA-2 and repression of TGF-β signaling. *Cancer Sci*. 2008;99(7):1407–1413.
46. Radtke F, et al. Deficient T cell fate specification in mice with an induced inactivation of NOTCH1. *Immunity*. 1999;10(5):547–558.
47. Inlay MA, et al. Identification of multipotent progenitors that emerge prior to hematopoietic stem cells in embryonic development. *Stem Cell Reports*. 2014;2(4):457–472.
48. Nguyen PD, et al. Haematopoietic stem cell induction by somite-derived endothelial cells controlled by meox1. *Nature*. 2014;512(7514):314–318.
49. Adamo L, et al. Biomechanical forces promote embryonic haematopoiesis. *Nature*. 2009;459(7250):1131–1135.
50. North TE, et al. Hematopoietic stem cell development is dependent on blood flow. *Cell*. 2009;137(4):736–748.
51. Fulton D, et al. Regulation of endothelium-derived nitric oxide production by the protein kinase AKT. *Nature*. 1999;399(6736):597–601.
52. Clements WK, Kim AD, Ong KG, Moore JC, Lawson ND, Traver D. A somitic Wnt16/NOTCH pathway specifies haematopoietic stem cells. *Nature*. 2011;474(7350):220–224.
53. Kim AD, et al. Discrete NOTCH signaling requirements in the specification of hematopoietic stem cells. *EMBO J*. 2014;33(20):2363–2373.
54. Kobayashi I, et al. Jam1a-Jam2a interactions regulate haematopoietic stem cell fate through NOTCH signalling. *Nature*. 2014;512(7514):319–323.
55. Lawson ND, et al. NOTCH signaling is required for arterial-venous differentiation during embryonic vascular development. *Development*. 2001;128(19):3675–3683.
56. Quillien A, et al. Distinct NOTCH signaling outputs pattern the developing arterial system. *Development*. 2014;141(7):1544–1552.
57. Vooijs M, et al. Mapping the consequence of NOTCH1 proteolysis in vivo with NIP-CRE. *Development*. 2007;134(3):535–544.
58. Taylor E, Taoudi S, Medvinsky A. Hematopoietic stem cell activity in the aorta-gonad-mesonephros region enhances after mid-day 11 of mouse development. *Int J Dev Biol*. 2010;54(6–7):1055–1060.
59. Schmitt TM, Zuniga-Pflucker JC. T-cell development, doing it in a dish. *Immunol Rev*. 2006;209:95–102.
60. Hu Y, Smyth GK. ELDA: extreme limiting dilution analysis for comparing depleted and enriched populations in stem cell and other assays. *J Immunol Methods*. 2009;347(1–2):70–78.